

Metal-insulator transition in 2D: the role of interactions and disorder

George Kastinakis

Dept. of Chemical Engineering, University of Cambridge, Cambridge CB2 3RA, U.K.

*Institute for Electronic Structure and Laser (IESL), Foundation for Research and Technology - Hellas (FORTH),
Iraklio, Crete 71110, Greece**

(June 9, 2002)

We present a model for the metal-insulator transition in 2D, observed in the recent years. Our starting point consists of two ingredients only, which are ubiquitous in the experiments: Coulomb interactions and weak disorder spin-orbit scattering (coming from the interfaces of the heterostructures in question). In a diagrammatic approach, we predict the existence of a characteristic temperature $T_o = T_o(n, \omega_H)$, n being the density of carriers, and ω_H the Zeeman energy, below which these systems become metallic. This is in very good agreement with experiments, and corroborates the fact that varying n and ω_H are equivalent ways into/out of the metallic regime. The resistivity, calculated as a function of temperature and ω_H in the metallic state, compares favorably to experiment. We comment on the nature of the transition, and calculate the specific heat of the system.

PACS numbers: 71.30.+h, 72.10.Bg, 72.10.-d, 72.15.Rn

In the last years, a metal-insulator transition has been observed in 2D systems by Kravchenko et al.¹ and others - see e.g.². In high mobility heterostructures, for carrier densities n higher than a critical density $n_c \sim 10^{11} \text{cm}^{-2}$, and at appropriately low temperatures T , of a few degrees Kelvin at *most*, a transition into a metallic state is observed². Moreover, a sufficient increase of the Zeeman energy ω_H of the carriers, through an externally applied magnetic field H , takes the system back into the insulating state². Hamilton et al.³ and Pudalov et al.⁴ have shown that beyond a maximum characteristic n'_c there is a second metal to insulator transition. Further, in the metallic regime, the resistivity is usually fitted very well by the formula - e.g.^{5,2}:

$$\rho_{exp}(T) = \rho_o + \rho_1 \exp[-(T_*/T)^k] , \quad (1)$$

where ρ_o, ρ_1 and T_* depend on n . The exponent k is in the range 0.5 - 1, and is material-dependent.

Ilani et al.⁶ have shown that for $n < n_c$ the insulating state is spacially inhomogeneous. Here, we will not attempt to provide a description of the insulating state. We *only* give a mechanism for the transition and a description of the metallic state. These are based on strong spin-dependent particle-hole correlations, which arise for the appropriate range of n and ω_H , in the frame of a Fermi liquid formulation.

The experimental systems in question have two ubiquitous characteristics. The ratio of the Coulomb energy to the Fermi energy ϵ_F is typically in the range 4-40². The importance of interactions has been decisively demonstrated by Ilani et al.⁶ and Dultz and Jiang⁷, who probed the compressibility in the metallic regime, and found it in agreement with a many-body interacting picture. On the other hand, weak disorder spin-orbit scattering is inadvertently present, coming from the interfaces of the heterostructures in question. These two characteristics constitute our starting point. We note that magnetic spin disorder would have the same effect as spin-orbit disorder, in the frame of our model. Strong support for the role of spin-dependent scattering is provided by the expts. of Vitkalov et al.⁸, which show that spin up and down mobilities remain comparable for all H . This is naturally interpreted in terms of strong spin up and down mixing through disorder scattering. Moreover, Vitkalov et al.⁹ have provided evidence that the insulating state is ferromagnetic, also supported by^{10,11,12}. Further, Ilani et al.¹³ have demonstrated the existence of localized charged islands in the metallic phase, which can be magnetic. If this is the case, we can assume that these magnetic islands sit on top of the aforementioned spin-orbit impurities. Then the scattering strength of the impurities is enhanced and the metallic behavior more pronounced - c.f. e.g. eq. (6) for $T_o(n, \omega_H)$ etc.

In the foregoing, we consider the coupling U between opposite spin carriers, and we denote by

$$u \equiv U N_F , \quad (2)$$

the dimensionless coupling, N_F being the density of states at the Fermi level. As usual, we work in the regime $\epsilon_F \tau > 1$ ($\hbar = 1$), ϵ_F being the Fermi energy and τ^{-1} the total impurity scattering rate. As we have shown in¹⁴, in the presence of weak disorder, which includes *spin* scattering, the ladder diagrams in the particle-hole channel give rise to the propagators $A^j(q, \omega_m)$, $j = 0, \pm 1$, obeying the coupled Bethe-Salpeter equations $A^1 = U + U \mathcal{D}^1 A^1 + U \mathcal{D}^0 A^0$, $A^0 = U \mathcal{D}^0 A^1 + U \mathcal{D}^{-1} A^0$. The variables q, ω_m , which stand for the momentum and Matsubara energy difference between particle and hole lines respectively, were suppressed. \mathcal{D}^j are given by $\mathcal{D}^{\pm 1} = \mathcal{D}^{1, \pm 1}$, $\mathcal{D}^0 = [\mathcal{D}^{0,0} - \mathcal{D}^{1,0}]/2$, $\mathcal{D}^{j, m_j}(q, \omega_m) = N_F \{ D q^2 + j 4 \tau_S^{-1} / 3 \} / \{ D q^2 + j 4 \tau_S^{-1} / 3 + |\omega_m| - i m_j \omega_H \}$, with τ_S^{-1} the total spin scattering rate and D the diffusion constant.

What turns out to be of interest here, is the "dynamic limit" $Dq^2 < \omega_m$, where the solution of these eqs. is¹⁴ $A^j(q, \omega_m) = K_{uj}/[A_u Dq^2 + B_u |\omega_m| + C_u]$, with

$$\begin{aligned} A_u &= 12 - 20u + 15u^2/2 + 6\Omega_H^2, \quad B_u = 4 - 6u + 3u^2/2 + 9\Omega_H^2/4, \\ C_u &= r[1 - 2u + 3u^2/4 + \Omega_H^2(1 - u^2/4)] \quad , \quad K_{u0} = Uru(1 + \Omega_H^2)/2 \quad , \quad K_{u1} = Ur(1 - u)(1 + \Omega_H^2) \quad , \end{aligned} \quad (3)$$

where $\Omega_H = \omega_H \tau_S$ and $r = 4\tau_S^{-1}/3$ ¹⁵.

We consider first the case with $\omega_H = 0$. For $u = 2/3 - 2$, $C_u < 0$. For $u \geq 0.845$, $B_u \leq 0$ as well. Then the ratio C_u/B_u is *negative* for $u = 2/3 - 0.845$, with $C_u < 0$ and $B_u > 0$. We interpret this as the onset of strong particle-hole correlations in the spin density channel. For sufficiently low temperatures

$$T < T_o(u, \omega_H) \equiv \frac{|C_u|}{2\pi B_u} \equiv \frac{\omega_o}{2\pi} \quad , \quad (4)$$

a *resonance* occurs, which we interpret as driving the second-order transition into the metallic regime - c.f. below. A finite ω_H shrinks the range of u , which allows for this effect, until for high enough ω_H C_u becomes positive definite, and there is *no* transition into the metallic state. The dependence of the transition temperature T_o on u - or equivalently the carrier density - and ω_H are in accordance with experiment^{3,4,16,2}. Of course, the value of u is determined through the bandstructure by the density n .

We note that additional insertions in the Bethe-Salpeter equations for A^j , such as self-energy diagrams, do not influence the existence of this resonance. We believe there is no magnetic or superconducting instability involved here, and thus the location of the pole of A^j on the imaginary energy axis is unphysical. In a different approach, Chamon et al.¹⁷ assume a paired state in the metallic phase (which, however, is not easy to quantify). In order to make progress, we assume that in the metallic phase the usual Fermi liquid picture continues to apply, but C_u acquires a small imaginary factor: $C_u \rightarrow C_u + id$, which moves the pole of A^j at a distance off the imaginary axis, thus yielding well-defined metallic contributions to the conductivity. d should satisfy the conditions $w \equiv [(2\sqrt{2\pi}K_{uj}^2 N_F^{3/2} \tau^{3/2} T \omega_o)/(d m A_u D \epsilon_F^2)] > 1$ (A) and $d = \pm d_o |C_u|^\xi T^\chi$ (B), with $0 \leq \xi \leq 1$, $0 \leq \chi \leq 1$ and $T^\chi d_o(T) \rightarrow 0$ for $T \rightarrow 0$, in order to yield physically meaningful contributions (the sign \pm corresponds to the position of A^j with regards to the main particle-hole lines, as shown in figs. 1-3). In fact, a finite d is consistent with the finite imaginary part of the dephasing rate for finite ω - c.f. e.g.¹⁸.

To calculate the conductivity using the renormalized A^j , we proceed as follows. First, relevant processes must take into account the resonance of $A^j(q, \omega)$. For this, diagrams, such as the ones in figs. 1-3, containing at least 2 $A^j(q, \omega)$'s with the *same* q and ω are needed in order to yield the enhancement factor w of (A) above, which then appears in the factors $gz_{1,2}$ and $zz_{1,2}$ of eq. (5). The diffuson $D_{q,\omega}$, in between, both provides essential T -dependence and separates the A^j 's from each other. Then the diagrams shown in figs. 1-3 yield the maximum contribution around a single diffuson $D_{q,\omega}$. The reasoning here is similar to a related, but different, calculation in¹⁴. Summing the infinite series shown in figs. 1-3 for $\omega_o < \tau^{-1} < \epsilon_F$ we obtain

$$M_\sigma = g \frac{[z_1 + z(z_1^2 + z_2^2)]F_1 + [z_2 + 2z(z_1 z_2)]F_2}{1 - z^2(z_1^2 + z_2^2)} \quad . \quad (5)$$

Here, $g = \frac{g_o}{2\pi\tau N_F}$, $g_o = \left\{ \frac{N_F^2 T \omega_o}{4m^* A_u D \epsilon_F^2 d} \right\}^2$, $z = g_o \left\{ \frac{4\pi\epsilon_F^2}{\Omega^3} \right\}^2 \left\{ 1 + \frac{1}{\Omega^2 \tau^2} \right\}$, m^* is the effective carrier mass, $\Omega = \tau^{-1} + \omega_o$, $z_1 = K_{u1}^4 + K_{u0}^4$, $z_2 = 2K_{u1}^2 K_{u0}^2$, $F_1 = \ln\left(\frac{2\pi T + T_1}{2\pi T}\right)$, $F_2 = \frac{1}{2} \ln\left(\frac{(2\pi T + T_1 + r)^2 + \omega_H^2}{(2\pi T + r)^2 + \omega_H^2}\right)$ and $T_1 = \tau^{-1}$.

Then we sum the infinite series, the n -th term of which contains n blocks M_σ in series, sandwiched between the current vertices of a conductivity bubble :

$$\sigma_M = \frac{2e^2}{m^2} \int d\vec{k} k_x^2 \frac{\Gamma^2 M}{1 - \Gamma M} \quad . \quad (6)$$

Here $M = \Gamma_1 - \Gamma\Gamma_2$, $\Gamma = G_R(k, \epsilon_F)G_A(k, \epsilon_F)$, $\Gamma_1 = aM_\sigma$, $\Gamma_2 = bM_\sigma$, with $a = \alpha\tau^2$, $b = 1/(2\pi\epsilon_F\tau)$, $\alpha = 1 - (2\tau)^2 \left(\frac{4}{9\tau_S^2} + \frac{1}{3\tau_S\tau_o} \right)$, $\tau_o^{-1} = \tau^{-1} - \tau_S^{-1}$ is the scattering rate due to non-magnetic impurities, and m the carrier mass. In this way we obtain a M -dependent formula for the total conductivity in the metallic regime :

$$\sigma = \sigma_o + \sigma_M = \frac{2N_F e^2 \epsilon_F \pi}{3mS} \left\{ \frac{y_+}{\sqrt{t^2 - y_+}} - \frac{y_-}{\sqrt{t^2 - y_-}} \right\} s_\sigma(T) \quad . \quad (7)$$

Here $y_{\pm} = (\Gamma_1 \pm S)/2$, $S = \sqrt{\Gamma_1^2 - 4\Gamma_2}$. σ_o is the Drude term. $s_{\sigma}(T)$ is a smooth analytic function, equal to 1 for $T \leq T_o$ and gradually vanishing for $T > T_o$ ¹⁹. Eq. (7) is a gauge-invariant approximation for the conductivity¹⁴.

The fit of eq. (7) to the activated exponential in T form for the resistivity of eq. (1), usually fit to the experimental data, is shown in fig. 4. We take $\chi = 1$ - which gives an excellent match with eq. (1) in the "high T " limit - $\xi = 0$ and $d_o = \text{const}$. We plot $\rho(H=0)/\rho_*$, where $\rho = 1/\sigma$ and $\rho_* = 3m\tau/(\pi e^2 N_F \epsilon_F)$. $s_{\sigma}(T) = 1$ for all T here. The overall variation of ρ/ρ_* within a given T range increases with u and g . Hence, an appropriate choice of these parameters yields a resistivity which appears practically constant - c.f. e.g. the experimental data in ref.²⁰ - although it has the same shape as the curves of fig. 4. Overall, the fit of eq. (7) is good. It can be seen that there is a discrepancy for low T . This is due to the fact that the series summed up corresponds to the "high T " limit of this theory, which is nevertheless *appropriate* for T even of the order of a few hundred mK. For the $T \rightarrow 0$ limit, another class of diagrams becomes dominant, such as the one shown in fig. 5. Analysis shows that this class contains *asymptotic series* (i.e. $\sum_n^{\infty} n! [\text{const.}/T]^n$), which cannot be formally summed, hence we cannot calculate σ_M in this limit. Nevertheless, we conjecture σ_M to be finite for $T \rightarrow 0$.

In fig. 6 we plot the magnetoresistance corresponding to eq. (7), as a function of (H/H_*) . The field at which $C_u = 0$ is $H_* = \sqrt{[1 - 2u + 3u^2/4]/(1 - u^2/4)}/(g_c \mu_B r)$, g_c the gyromagnetic ratio of the carriers and μ_B the Bohr magneton. Again, $s_{\sigma}(T) = 1$ for all T . The magnetoresistance for $H \rightarrow 0$ scales like (H^2/T^{γ}) , where $\gamma \simeq 1.7 - 1$ for the parameter set (1) of fig. 4 - for $T > 0.7$ K $\gamma = 1$. For the parameter set (2), $\gamma \sim 0.9$. The typical range of values of γ are in marked difference from $\gamma_W = 2$ expected from the conventional weak disorder magnetoresistance, but compare very favorably with expts.²¹.

Turning to the conventional weak disorder conductivity contributions in the presence of finite M , it is easy to see that they can typically be written as

$$\sigma_W = \frac{2e^2}{m^2} \int d\vec{k} k_x^2 \frac{\Gamma^2 W}{(1 - \Gamma M)^2} , \quad (8)$$

in a manner analogous to eq. (6) - but note the square in the denominator of eq. (8). W stands for any such diagrammatic contribution, with or without interactions. E.g. the conventional weak localization correction corresponds to $W \equiv -C$, $C_{q,\omega}$ being the Cooperon²². From eqs. (6) for σ_M and (8) for σ_W , we obtain $\sigma_W \ll \sigma_M$ for $W \ll M$. We believe this to be the explanation behind the negligible weak localization etc. contributions observed in a number of experiments^{20,23}. The same is true for the Hall coefficient as well, e.g.²³. Note that, with increasing H , M decreases, and the weak disorder σ_W is enhanced, as seen in²³. On the other hand, finite but small weak disorder contributions, which behave like $-\ln(T)$ in 2D^{22,2}, have also been observed in^{24,25}. In the frame of our model, it is reasonable to expect that at exponentially small T σ_W should dominate over σ_M , and hence drive the system into the insulating regime. In that case, we would *not* have a $T = 0$ quantum metal-insulator phase transition. However, there are two caveats here. Kopietz has shown that the quasiparticle weight vanishes for $T \rightarrow 0$ ²⁶, in an interacting 2D Fermi gas with spinless disorder - the case with spin disorder remaining unresolved. Moreover, the well known Kohn-Luttinger instability to a superconducting phase may also interfere in the limit $T \rightarrow 0$. Hence the fate of the metallic state for $T \rightarrow 0$ is an open question.

Based on our model, we evaluate the specific heat δC_V of the carriers, corresponding to the same processes yielding σ_M in eq. (6). The free energy is $F_M = N_F \omega_o \tau K \ln\{(\epsilon_F - K\tau)/(\epsilon_F + K\tau)\} s_F(T)$, with $K = \sqrt{g[z_1 F_1 + z_2 F_2]}$ and $\delta C_V = -T \partial^2 F_M / \partial T^2$. Here we took into account the diagrams of figs. 1 and 2, but not of fig. 3. $s_F(T)$ has the same properties as $s_{\sigma}(T)$ above. As before, this result is not valid for $T \rightarrow 0$. We note the pronounced H dependence of δC_V .

To summarize, we have shown that interactions and spin disorder can drive the second order metal-insulator transition observed in 2D systems. The transition arises from the onset of strong spin-density correlations, for a restricted range of the carrier density, the Zeeman energy and the temperature. We obtain good agreement with the experimentally determined dependence of the conductivity on these parameters.

I have enjoyed discussions and/or correspondence with P. Kopietz, P.T. Coleridge, A. Hamilton, D.E. Khmel'nitskii, S.V. Kravchenko, V. Senz and S. Vitkalov. I acknowledge the hospitality of V.S. Vassiliadis in Cambridge.

* Current address. E-mail : kast@iesl.forth.gr

- ¹ S.V. Kravchenko et al., Phys. Rev. B **50**, 8039 (1994); S.V. Kravchenko et al., Phys. Rev. B **51**, 7038 (1995); S.V. Kravchenko et al., Phys. Rev. Lett. **77**, 4938 (1996).
- ² E. Abrahams, S.V. Kravchenko & M.P. Sarachik, Rev. Mod. Phys. **73**, 251 (2001).
- ³ A.R. Hamilton et al., Phys. Rev. Lett. **82**, 1542 (1999).
- ⁴ V.M. Pudalov, G. Brunthaler, A. Prinz & G. Bauer, Phys. Rev. B **60**, R2154 (1999).
- ⁵ V.M. Pudalov et al., JETP Lett. **66**, 175 (1997).
- ⁶ S. Ilani, A. Yacoby, D. Mahalu, H. Shtrikman, Phys. Rev. Lett. **84**, 3133 (2000).
- ⁷ S.C. Dultz, H.W. Jiang, Phys. Rev. Lett. **84**, 4689 (2000).
- ⁸ S.A. Vitkalov et al., cond-mat/0008456.
- ⁹ S.A. Vitkalov et al., Phys. Rev. Lett. **87**, 086401 (2001).
- ¹⁰ A.A. Shashkin, S.V. Kravchenko, V.T. Dolgoplov & T.M. Klapwijk, Phys. Rev. Lett. **87**, 086801 (2001).
- ¹¹ V.M. Pudalov et al., Phys. Rev. Lett. **88**, 196404 (2002).
- ¹² S.V. Kravchenko, A.A. Shashkin & V.T. Dolgoplov, cond-mat/0106056.
- ¹³ S. Ilani, A. Yacoby, D. Mahalu & H. Shtrikman, Science **292**, 1354 (2001).
- ¹⁴ G. Kastinakis, Europhys. Lett. **42**, 345 (1998).
- ¹⁵ The opposite limit $Dq^2 > \omega$ does not yield the effect sought for, despite $B_u < 0$ for $1 < u < 1.2$.
- ¹⁶ M.P. Sarachik, S.V. Kravchenko, Proc. Natl. Acad. Sci. USA **96**, 5900 (1999).
- ¹⁷ C. Chamon, E.R. Mucciolo & A.H. Castro Neto, Phys. Rev. B **64**, 245115 (2001).
- ¹⁸ A. Völker & P. Kopietz, Phys. Rev. B **65**, 045112 (2002).
- ¹⁹ $s_\sigma(T)$ appears as follows. The resonances of the pole of $A^j(q, \omega_m)$ occur at $T = T_m \equiv T_o/m$, with $m = 1, 2, 3, \dots$. This would yield a metallic state for this discrete set of T_m 's only. However, due to disorder inhomogeneity, both u and τ_S^{-1} vary in space, which we account for via an appropriate distribution of T_o , centered e.g. at T_o^* . The latter yields a *continuum* of relevant T_m 's, i.e. a metallic state for $T < T_o^*$ weighted by $s_\sigma(T)$.
- ²⁰ S.V. Kravchenko & T.M. Klapwijk, Phys. Rev. Lett. **84**, 2909 (2000).
- ²¹ V.M. Pudalov et al., cond-mat/0103087; V.M. Pudalov et al., cond-mat/0205449.
- ²² B.L. Al'tshuler & A.G. Aronov, in *Electron-Electron Interactions in Disordered Systems*, A.L. Efros, M. Pollak, Eds. (Elsevier, Amsterdam 1985).
- ²³ P.T. Coleridge, A.S. Sachrjda & P. Zawadzki, cond-mat/9912041.
- ²⁴ M.Y. Simmons et al., Phys. Rev. Lett. **84**, 2489 (2000).
- ²⁵ V. Senz et al., Phys. Rev. Lett. **85**, 4357 (2000).
- ²⁶ P. Kopietz, Phys. Rev. Lett. **81**, 2120 (1998); also L. Bartosch & P. Kopietz, cond-mat/0108463.

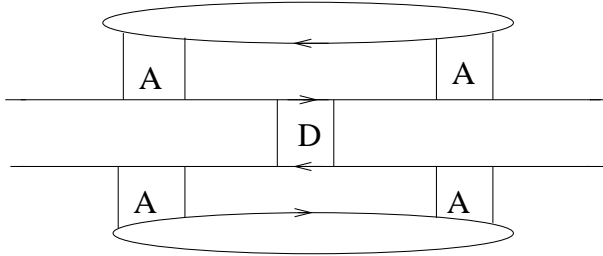


Fig. 1

The basic (lowest order) diagrammatic block for M_σ . $D_{q,\omega}$ is the diffuson²² and A the renormalized propagator of eqs. (3). All the appropriate spin structure diagrams are kept.

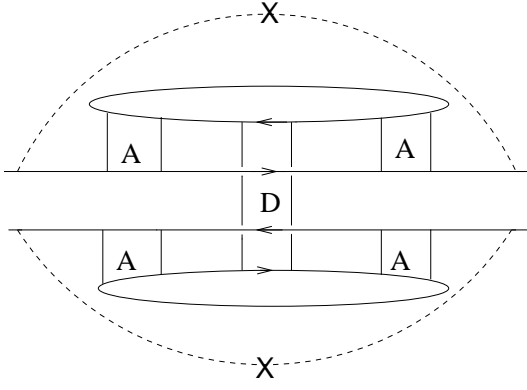


Fig. 2

Variations on the diagram of fig. 1. Here the diffuson connects the bubble lines. One or two impurity scattering line(s) decorate the main upper and/or lower line(s).

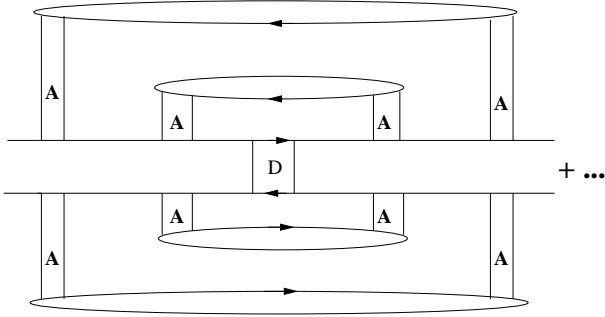


Fig. 3

The second order term of the diagrams of the type of figs. 1 and 2. To obtain M_σ in eq. (5), we sum the respective infinite series, which contains all possible variations of the diagrams shown in figs. 1-3.

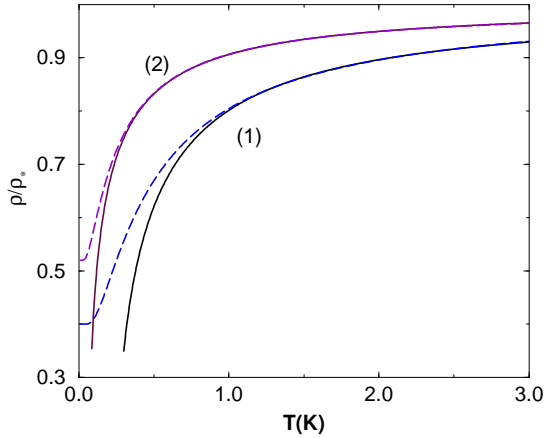


Fig. 4

Fit of eq. (7) - continuous lines - to the experimentally determined resistivity form of eq. (1) - dashed lines. Here $H = 0$ and $\rho_* = 3m\tau/(\pi e^2 N_F \epsilon_F)$. $\chi = 1$ and $\xi = 0$. Both curves (1) and (2) have $u=0.84$, $r = \tau^{-1} = 2$ K, and only differ by the ratio $g^{(1)}/g^{(2)} = 2$. The parameters of eq. (1) are $(\rho_o/\rho_*) = 0.40/0.52$, $(\rho_1/\rho_*) = 0.61/0.477$, $T_* = 0.42/0.21$ K and $k = 1$, for the curves (1) and (2) respectively.

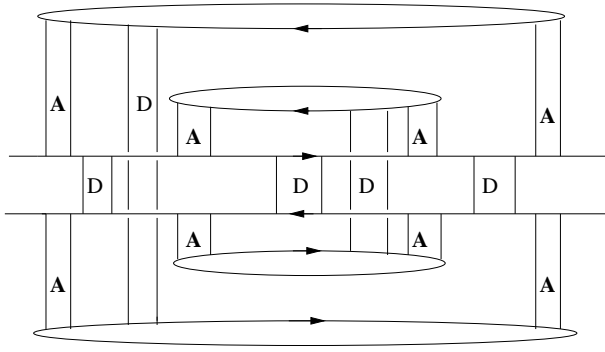


Fig. 5
A typical diagram of the dominant class in the $T \rightarrow 0$ limit.

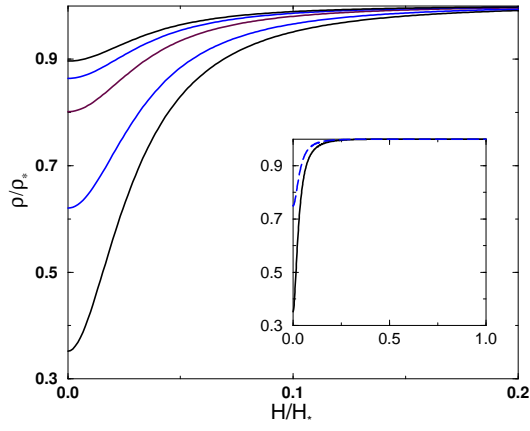


Fig. 6
Magnetoresistance from eq. (7), for the parameter set (1) of fig. 4. H_* is given in the text. The curves bottom to top correspond to $T=0.3, 0.5, 1, 1.5$ and 2 K. We note that $\rho/\rho_* = 1$ implies $M = 0$. The full curves to $H = H_*$ for $T = 0.3$ K are shown in the inset, the dashed line corresponding to the parameter set (2) of fig. 4.